European Journal of Pharmaceutics and Biopharmaceutics 136 (2019) 131–137

Contents lists available at ScienceDirect

European Journal of Pharmaceutics and Biopharmaceutics

journal homepage: www.elsevier.com/locate/ejpb

Research paper

Screening a trace amount of pharmaceutical cocrystals by using an enhanced nano-spot method

Yuta Tanabe[a], Yusuke Maeno[b], Kento Ohashi[a], Hiroshi Hisada[a], Anjan Roy[c], James Carriere[c], Randy Heyler[c], Toshiro Fukami[a,*]

[a] Department of Molecular Pharmaceutics, Meiji Pharmaceutical University, 2-522-1 Noshio, Kiyose, Tokyo 204-8588, Japan
[b] Analysis Research Department, Nissan Chemical Corporation, 2-10-1 Tsuboi-nishi, Funabashi, Chiba 274-8507, Japan
[c] Coherent Inc., 850E, Duarte Road, Monrovia, CA 91016, USA

ARTICLE INFO

Keywords:
Cocrystal
Screening
Low-frequency Raman spectroscopy
Polymorphism
Solvent vapor exposure

ABSTRACT

Cocrystallization is an attractive and promising technology that can improve the physical properties of formulations of active pharmaceutical ingredients (APIs). We have developed a "nano-spot method" that can evaluate the crystalline form on the nanogram scale. In this study, the following studies were performed to obtain versatile and comprehensive improvements to the nano-spot method: modification of the sample solution, application of solvent vapor exposure to attempt the precipitation of various states of crystals, and adoption of low-frequency Raman spectroscopy. Carbamazepine was used as a model API and cocrystallization screening was examined with 12 cocrystal formers (coformers). In the case of combinations that are already known to form cocrystals, spectra similar to those of previously reported cocrystals or new spectra were obtained. It was considered that the reported cocrystals or new polymorphs were obtained. In contrast, in the case of the combination which has been reported not to form a cocrystal, the spectra were consistent with that for the physical mixture of API and coformer, suggesting that a cocrystal also did not form in this screening. In addition, the newly adopted low-frequency Raman spectroscopy enabled the high-sensitive detection of the crystalline form.

1. Introduction

Recently, in the pharmaceutical industry, the issue related to the poor water solubility of active pharmaceutical ingredients (APIs) has received increasing attention [1]. Lately, the design of pharmaceutical cocrystal has attracted attention as a technique to improve the solubility of API. A cocrystal is defined as a crystalline solid with two or more molecules having a certain stoichiometric ratio with a noncovalent bond, excluding simple salts or solvates [2,3]. There are a number of reports indicating that cocrystals can improve the solubility or bioavailability compared to APIs alone [4–7].

A cocrystal is prepared by various ways from the API and excipient (coformer), which has no medicinal efficacy [3,8–10]. In the development of pharmaceutical cocrystals, a suitable coformer that is expected to improve the physical properties of APIs should be selected. It is recommended that the candidate coformers should be chosen from not only excipients that have already been used as drugs commercially but also compounds listed in GRAS (Generally Recognized As Safe) or EAFUS (Everything Added to Food in the United States) [11]. Therefore, the options for coformers are notably diverse. Conversely, in the early stage of drug discovery and development, the amount of API that can be used for the solid form screening is very limited because the synthetic process has not been established, and in turn, the amount of API synthesized is relatively low and expensive. For these reasons, an efficient method for exploring coformers is required. Within such circumstances, some high-throughput screening methods for cocrystals using multiwell plates have been reported [12–15]. These papers reported that the API and each coformer are mixed in 96-well plates and cocrystalized in various ways, and the prepared specimens (cocrystals) are evaluated by powder X-ray diffractometry (PXRD), Raman spectroscopy, and differential scanning calorimetry (DSC). Therefore, several milligrams to hundreds of milligrams of the sample volume per measurement are required.

In a previous study, we have developed and reported a nano-spot method as an efficient microanalysis method for exploring pharmaceutical cocrystals [16]. The nano-spot method is a technique to evaluate precipitated microcrystals on a hydrophobized glass plate using Raman spectroscopy after the sample solution is spotted by a microsyringe. It has been suggested that the method has the possibility to explore cocrystals at the nanogram scale. However, some APIs cannot

---

* Corresponding author.
E-mail address: fukami@my-pharm.ac.jp (T. Fukami).

https://doi.org/10.1016/j.ejpb.2019.01.018
Received 1 October 2018; Received in revised form 10 January 2019; Accepted 16 January 2019

Table 1
Reagents used for solvent consideration.

APIs		
Acetazolamide	Caffeine	Carbamazepine
Chlorpropamide	Clarithromycin	Furosemide
Griseofulvin	Haloperidol	Indomethacin
Ketoprofen	Mefenamic acid	Phenytoin
Sulindac		
Carboxylic acids		
4-Aminobenzoic acid	Adipic acid	Anthranilic acid
Benzoic acid	Camphoric acid	Fumaric acid
Glutaric acid	Hydroxybenzoic acid	Isophthalic acid
Maleic acid	Malonic acid	Mandelic acid
Oxalic acid	Phthalic acid	Salicylic acid
Succinic acid		

Table 2
Reagents used for exploratory screening of CBZ cocrystal.

Compound Name	Abbreviation	Supplier
4-Aminobenzoic acid	ABA	TCI
Adipic acid	ADI	Wako
Benzoic acid	BA	Wako
Fumaric acid	FMA	Wako
Glutaric acid	GLA	TCI
Maleic acid	MLA	Wako
Malonic acid	MLN	Wako
Nicotinamide	NCT	TCI
Oxalic acid	OXA	Wako
Saccharin	SAC	Wako
Succinic acid	SUC	Wako
Picolinamide	PA	TCI

be applied in this method because of their low solubility in ethanol (EtOH), which is used as a solvent, and because agglomerated crystals make it difficult to acquire the Raman spectra. In this study, a small amount of dimethyl sulfoxide (DMSO) was added to EtOH with the purpose of reducing and homogenizing the diameter of the crystals and thereby enhancing the applicable API lineup.

Since the detection of all possible crystalline forms is important in the solid form screening, many crystallization conditions should be tested. Therefore, solvent vapor exposure was applied as a method for examining a large number of crystallization conditions on a single plate. In other words, it has been reported the solvent vapor exposure can drive the transition of crystalline form or the formation of a cocrystal [17,18], and we also expected to obtain the different crystalline form. Furthermore, low-frequency region Raman spectroscopy (LF Raman) was newly used as an analysis method in addition to mid-frequency Raman spectroscopy (mid Raman), the distinctive spectrum peaks of which are derived from the bond vibrations between atoms that provide information on the chemical structure of the compounds. Conversely, LF Raman is characterized by specifically obtaining information on the crystal forms from the lattice vibration-derived spectra of the crystals [19,20]. The low-frequency vibrational spectroscopy such as LF Raman and terahertz pulsed spectroscopy was reported to be able to differentiate the polymorphs or solid state of API (crystal or amorphous) [21–23]. In addition, these phonon spectra could be predicted by lattice dynamics calculation [24]. Since we have reported the identification of polymorphs and monitoring of the crystalline form transition by LF Raman [25–27], this work presented an opportunity to examine sensitivity of LF Raman in detecting cocrystal formation.

2. Materials and methods

2.1. Hydrophobization of the quartz plate

A quartz plate, which has less effect on the Raman spectra, was used for spotting the sample solution. The surface of the plate was hydrophobized by the fluorochemical hydrophobing reagent Novec1720 (3 M, Tokyo, Japan). The reagent was applied to the plate surface by spin coating and dried at 100 °C for 15 min before use. A 2 × 2 mm square scale was attached to the back of the plate, which was used as a guide for the spotting position, and the sample solution was spotted to the center of the square. A digital microscope (Dino-Lite Pro 2 Premier, AnMo Electronics Corporation, Taiwan) was used to observe while spotting since the spotting operation was difficult to visualize.

2.2. Comparison of the crystallization zone diameter

EtOH and DMSO (Wako: FUJIFILM Wako Pure Chemical Corp., Osaka, Japan) were used as sample solvents. Thirteen APIs and 16 carboxylic acids were used to compare the diameter of the precipitated crystals (Table 1). Each compound was dissolved in EtOH and a mixture of EtOH/DMSO (99/1), respectively, to prepare a 1 mg/mL solution. 50 nL of these solutions were spotted with a microsyringe on the hydrophobized plate. The droplets were dried under ambient temperature or via lyophilization to precipitate the crystals. The resulting crystals were observed with a polarizing microscope to measure the diameter, and the mean diameters and standard deviations were calculated (n = 4).

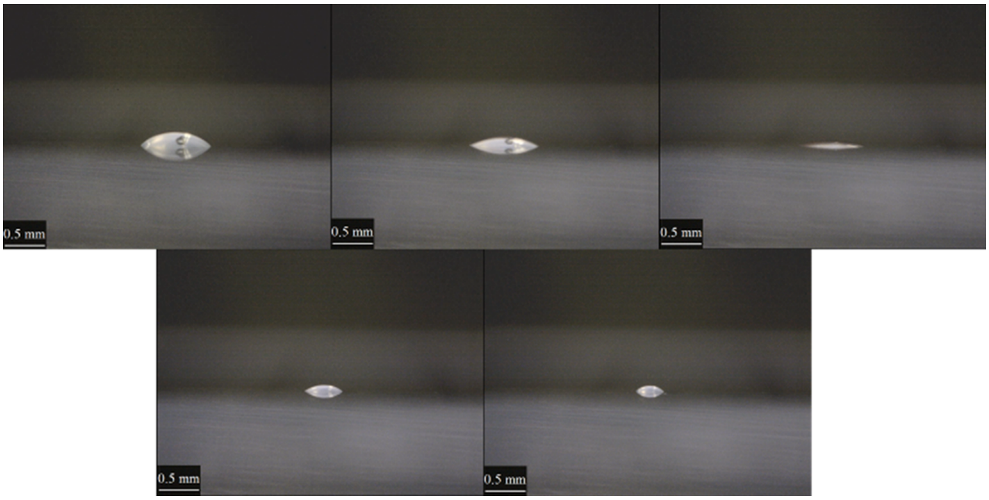

Fig. 1. Phase of evaporating droplet. (a)–(c) After spotting, the EtOH volatilized in advance and (d)–(e) and a smaller DMSO droplet was formed.

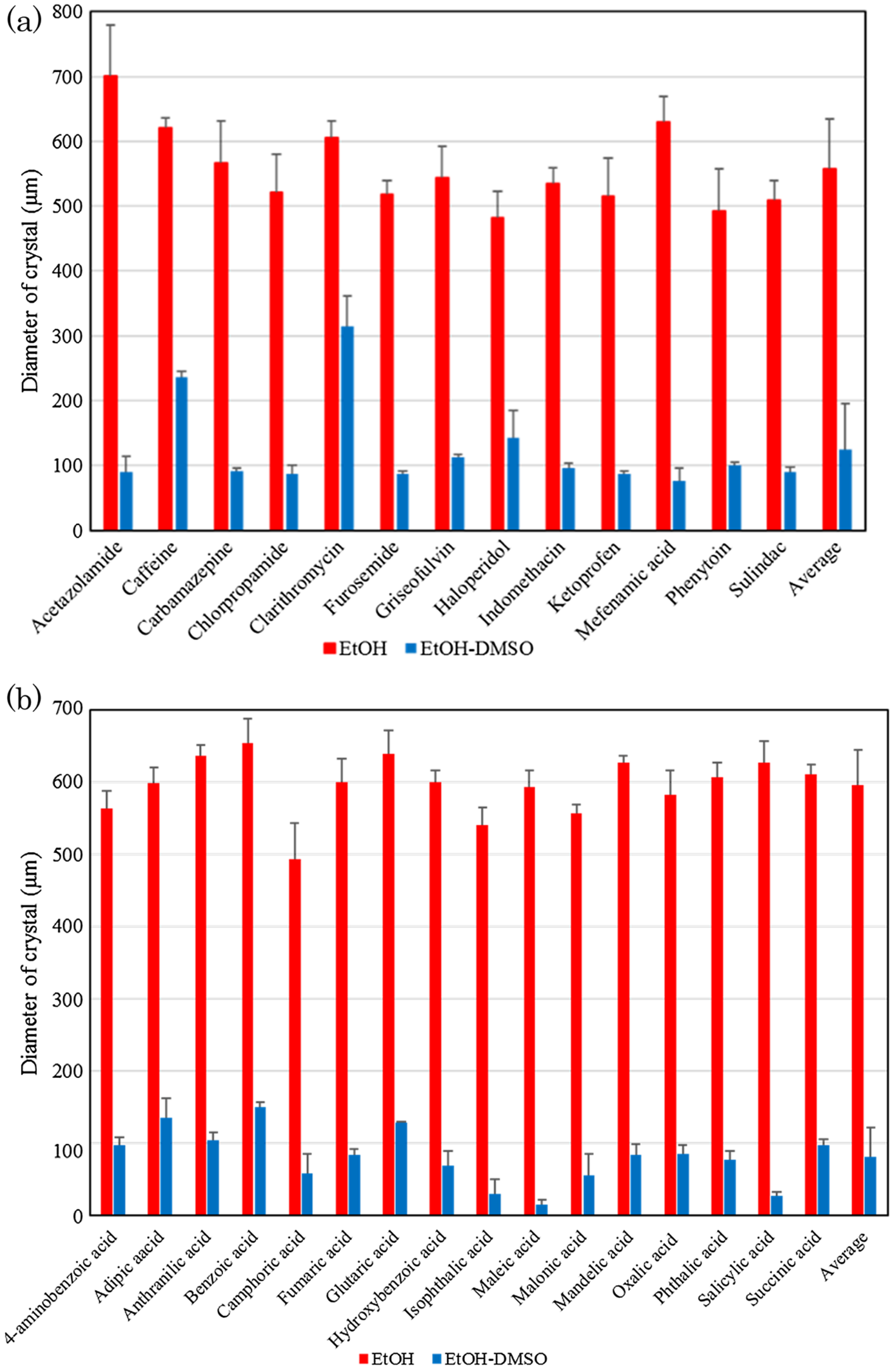

Fig. 2. Diameter of (a) API and (b) carboxylic acid crystals. The error bar indicates standard deviation (n = 4).

2.3. *Exploratory screening for CBZ cocrystal*

2.3.1. *Sample preparation*

Carbamazepine (CBZ) (TCI: Tokyo Chemical Industry Co., Ltd., Tokyo, Japan) as a model API and 12 coformers were selected (Table 2). It has been reported that 11 coformers formed cocrystals with CBZ, while PA did not form a cocrystal [28–30]. The sample solution was prepared by dissolving totally 20 mg of CBZ and each coformer (1:1 M ratio), which was weighed by using accurate analytical balance, in 10 mL of EtOH/DMSO (99/1). 50 nL of these solutions were spotted on the hydrophobized quartz plate by a microsyringe and the plate was lyophilized.

2.3.2. *Solvent vapor exposure*

Five solvents were selected as exposing solvents: acetone (ACE), ethyl acetate (AcOEt), chloroform (CLF), acetonitrile (MeCN) and tetrahydrofuran (THF) (from Wako). The sample plate and 9 mL of each solvent in a beaker were placed in a container and stored for 4 days at a constant temperature of 40 °C. Another plate was also stored at the same condition in the absence of an exposure solvent for comparison.

2.3.3. *Raman spectroscopy*

The Raman spectra were acquired after lyophilization and after solvent vapor exposure treatment. A Raman Workstation (Kaiser Optical Systems Inc., MI, USA) was used for the mid Raman measurement, and an XLF-CLM module (ONDAX Inc., CA, USA) was attached to

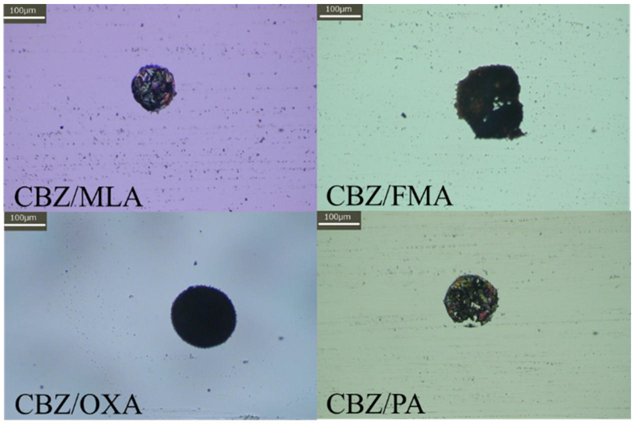

Fig. 3. Typical examples of CBZ/coformers microcrystals precipitated on the plate.

the Workstation for the LF Raman measurement. The excitation laser wavelengths for the measurements were 785 nm for mid Raman and 976 nm for LF Raman, and the measurement condition was 10 s of exposure and one accumulation.

2.4. Preparation of standard cocrystals (Ref)

Standard cocrystals (Ref) were prepared to compare the obtained microcrystals on the plate. CBZ/ADI, CBZ/BA, CBZ/FMA, CBZ/GLA, CBZ/MLA, CBZ/MLN, CBZ/SUC were prepared by slurry or solvent evaporation method according to Childs' report [28]. The other cocrystals were prepared according to Weyna's report [29]. The prepared cocrystals were confirmed by PXRD (MiniFlex600, Rigaku Corp., Tokyo, Japan). Afterwards, mid and LF Raman measurements were performed under the conditions shown in 2-3-3.

3. Results and discussion

3.1. Comparison of the crystallization zone diameter

In the previously reported nano-spot method, EtOH was used as the test solution, but the zone diameters of the precipitated crystals tended to increase in the case of hydrophobic APIs. Even if the same sample volume was spotted, the thickness of the precipitated crystals became thinner as the diameter became larger, and finely focused adjustment was required in the microscopic Raman measurement; otherwise, Raman spectra with very weak intensities were acquired. Then, by mixing a small amount of DMSO with a larger surface tension than EtOH, the reduction of the droplet diameter and the precipitated crystallization zone diameter was attempted. When the EtOH/DMSO mixture was spotted on the plate, the EtOH that made up most of the mixed solvent volatilized rapidly, and with the gradual increase of the DMSO proportion, the contact angle increased sharply, and a minute droplet, probably composed of DMSO and a trace amount of EtOH, was formed (Fig. 1).

The mean and standard deviation of the crystalline diameters were remarkably decreased by using the EtOH/DMSO (99/1) mixture in both cases of APIs and carboxylic acids (Fig. 2). Although the hydrophilicity or hydrophobicity of the solute was directly reflected by the droplet size in the previous study using EtOH alone [16], an interaction between the solution and the surface of the hydrophobized plate was suggested to become dominant after adding DMSO. Therefore, using the EtOH/DMSO (99/1) mixture as the sample solution could decrease the diameters of each API and carboxylic acid, utilizing the property of DMSO as a good solvent for dissolving various compounds in comparison to EtOH alone.

3.2. Exploratory screening for CBZ cocrystal

3.2.1. Precipitation of microcrystal

As a result of the studies of the sample concentration and the mixing proportion of EtOH and DMSO for the precipitation condition of CBZ, 162 ± 45 μm-diameter and theoretically 100 ng CBZ-coformer crystals could be obtained when the concentration was 2.0 mg/mL and the ratio of EtOH/DMSO was 99/1 (Fig. 3). The Raman spectra of these crystals were also able to be acquired, particularly the LF Raman spectra, which had less baseline drift than the mid Raman spectra, and it was easy to discriminate the shifted peaks. Fluorescence affected the baseline and the peak intensity of some mid Raman spectra, which made it difficult to compare their spectra in some conditions. Accordingly, the difference of the shifted peaks could be clearly judged by comparing the LF Raman spectra prior to mid Raman in this improved method.

3.2.2. Changes in the Raman spectra after solvent vapor exposure

The microcrystals on the plate were exposed to solvent vapor, and mid and LF Raman spectra were acquired. The spectra of CBZ/MLA, CBZ/FMA, CBZ/OXA, and CBZ/PA exposed to ACE vapor are shown in Fig. 4 as representative examples. The Raman spectra of CBZ/MLA did not change after lyophilization or after exposure to ACE vapor (Fig. 4a). The spectra were consistent with the reference cocrystal (Ref) after lyophilization, suggesting that Ref was formed on the plate. Because there are two polymorphs of the cocrystal (Form A (Ref A) and Form B (Ref B)) in CBZ/FMA, the spectra obtained by solvent vapor exposure were compared with them (Fig. 4b). In the mid Raman spectrum, a new peak appeared at approximately 1700 cm^{-1}, which was consistent with the spectrum of the separately prepared Ref B, comparing after lyophilization and after ACE vapor exposure. In the LF Raman spectra, new peaks appeared at approximately 25, 39, 62, 78, and 112 cm^{-1}, and they were also consistent with the spectrum of Ref B. From these results, it was considered that the crystal on the plate was transformed to Ref B by the solvent vapor. On the other hand, in the case of CBZ/OXA, a new peak was observed at approximately 1700 cm^{-1} after ACE vapor exposure in the mid Raman spectrum, but this peak was not observed in the spectrum of the Ref, single CBZ, or OXA. This suggested that a new crystalline form was obtained (Fig. 4c). Referring to the LF Raman spectrum, although the peak at approximately 25 cm^{-1} was consistent with the peak of Ref, a new peak appeared at approximately 48 cm^{-1}, and a peak at approximately 110 cm^{-1}, which is similar to the peak of CBZ form I, was observed. It was suggested that the spectrum was a mixture of the new crystalline form, Ref, and CBZ form I. In contrast to these results, in the case of CBZ/PA, which has been reported not to form a cocrystal [26], no spectral changes in the mid and LF Raman spectra were observed after exposing to solvent vapor (Fig. 4d). In addition, the wavenumbers of the acquired peaks obtained were consistent with the spectra of the physical mixture (PM) of CBZ and PA. Therefore, it was confirmed that a cocrystal or a new crystalline form did not form, and the spectra did not change from that of the PM of CBZ and PA when using this method.

All of the evaluated results and spectra acquired in this study are shown in Table 3 and supporting information (Fig. S1). In Table 3, Ref indicates that the acquired spectra were consistent with that of a separately prepared standard cocrystal, and NP indicates that new peaks, which were not found in the standard cocrystal, CBZ and coformer, were observed. The colored cells also show that the solvent vapor exposure altered the LF Raman spectra from after lyophilization. The peaks derived from Ref, which has been reported to form a cocrystal, could be observed in all combinations of CBZ and coformers used in this study, where the solvent vapor exposure was utilized as preparation method. These results are reasonable because the solvents for vapor exposure that we chose were the same as in the Childs' report for preparing the standard cocrystal (except for CBZ/FMA form A) [24]. Additionally, for almost all combinations (9 out of the 11 combinations), the new LF Raman spectra differed from that of the API or

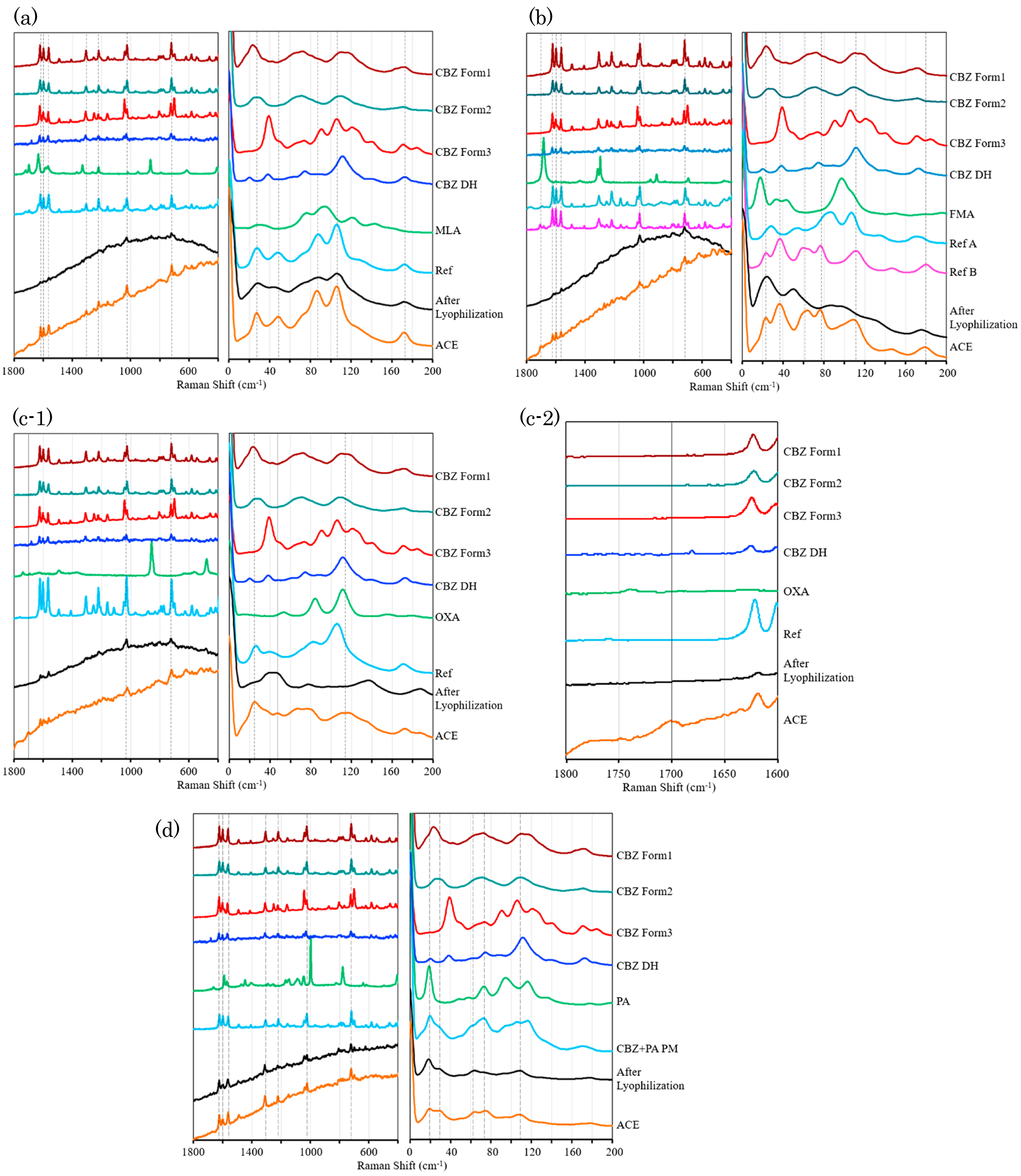

Fig. 4. Mid Raman (left) and LF Raman (right) spectra of (a) CBZ/MLA, (b) CBZ/FMA, (c) CBZ/OXA, and (d) CBZ/PA, respectively. “CBZ Form1-3” and “DH” indicate the polymorphs of CBZ and dihydrate, respectively. Black and orange spectra were collected after lyophilization and acetone (ACE) vapor exposure treatment, respectively. The dashed line indicates the distinctive peaks of each ACE spectrum, and the solid line indicates the Raman shift where the new peak appears in the ACE spectra. (c-2) Expanded mid Raman spectrum between 1600 and 1800 cm^{-1}. The new peak appeared at approximately 1700 cm^{-1}. (d) “PM” indicates the physical mixture of CBZ and PA.

coformer, due to the new peaks derived from the reported cocrystal polymorphs or new cocrystal polymorphs. CBZ has been reported to form four crystalline polymorphs and various cocrystals due to its good symmetrical structure consisting of aromatic rings and an amide [28]. To confirm whether a new crystalline phase was formed by using a typical analytical method, such as PXRD, is difficult in this study because the sample volume was 100 ng. However, these spectral changes might be false positives under some conditions e.g. crystalline

Table 3
Entire result of CBZ cocrystal screening.

API/ coformer	Solvent					
	None	ACE	THF	CLF	MeCN	AcOEt
CBZ/ABA	▨ NP	▨ NP	▨ NP	NP/Ref/ CBZ3	NP/CBZ3/ ABA	▨ NP
CBZ/ADI	▨ NP/Ref	NP/Ref	Ref	Ref	Ref	Ref
CBZ/BA	▨ NP/Ref	▨ NP/Ref	NP/Ref	▨ NP/Ref	▨ CBZ2	▨ NP/Ref
CBZ/FMA	NP	▨ Ref	▨ Ref/FMA	▨ Ref/FMA	▨ Ref/FMA	▨ Ref
CBZ/GLA	NP/Ref/ CBZ/GLA	▨ NP/CBZ3	▨ NP/Ref	NP/Ref/ GLA	▨ CBZ2	NP/Ref/ GLA
CBZ/MLA	Ref	Ref	Ref	Ref	Ref	Ref
CBZ/MLN	Ref	Ref	Ref	Ref/CBZ3	Ref	Ref
CBZ/NCT	NP/Ref	▨ Ref/NCT	▨ NP/Ref	▨ Ref	Ref	Ref
CBZ/OXA	▨ NP/Ref	▨ NP/Ref/ CBZ1	▨ NP/Ref	▨ NP/Ref	▨ Ref	▨ Ref/CBZ2
CBZ/SAC	▨ NP/Ref/ CBZ2	NP/Ref/ CBZ2	NP/Ref/ CBZ2	NP/Ref	▨ NP/Ref/ CBZ2/CBZ3	NP/Ref/ SAC
CBZ/SUC	NP/Ref	NP/Ref	Ref	Ref/SUC	Ref	▨ Ref
CBZ/PA	CBZ2/ CBZ3/PA	CBZ2/ CBZ3/PA	CBZ2/ CBZ3/PA	CBZ2/ CBZ3/PA	CBZ2/ CBZ3/PA	CBZ2/ CBZ3/PA

"Ref" indicates that the LF Raman spectrum was consistent with standard cocrystal.
"NP" indicates that new peak which is not consistent with CBZ, coformer, and standard cocrystal was observed in the LF Raman spectrum.
Colored cell shows that the spectrum has changed upon the solvent vapor exposure when compared to After Lyophilization.

transition of simple API or coformer. Even if they indicated factors other than the formation of new crystal forms, they were considered to be at least suitable for exploratory cocrystal screening. This is also supported by the fact that no changes in the LF Raman spectra were observed after any solvent vapor exposure in the case of CBZ/PA. For reference, the results of the investigation of another API, acetazolamide, are shown in the supporting information (Fig. S2, Table S1).

Although the screening method using resonant acoustic mixing device developed by Nagapudi et al. [15] had high success rate and ease of scale-up, the amount of sample consumption was 6 mg per sample, which was much more than our method. In addition, the examination of the acceleration and mixing time is required depending on the compound because the process uses physical mixing by applying resonant acoustic energies. Additionally, in the report of Luu et al. [12], using an automated crystallization screening system is a great advantage, but the required sample amount is estimated to be approximately 1 mg per condition due to the evaluation by PXRD. Although there have been many reports on the exploration methods for cocrystals as described above, none of them has challenged the nanogram-scale evaluation such as ours. However, the advance of peripheral technologies as well as analytical instruments is remarkable, and the evaluation of physical properties via a trace amount becomes possible by combining both technologies. For example, applications to the screening of a polymer-drug solid dispersion using the automatic dispensing unit of an inkjet printer have been reported [31], and further development of the microanalysis of physical properties is expected.

4. Conclusions

In this study, we were able to improve the nano-spot method previously reported by (i) decreasing the diameter of the precipitated microcrystals by adding DMSO to the sample solvent, (ii) improving the specificity and sensitivity by using LF Raman spectroscopy, and (iii) diversifying the crystallization condition by solvent vapor exposure. These modifications allowed the method to be applied to more APIs and various crystallizing conditions, and the specific detection and evaluation could be achieved. Although the sample consumption increased from 10 ng per spot to 100 ng per spot compared to our previous report, it is still able to evaluate 10,000 conditions on a 1 mg scale. Therefore, a comprehensive examination of the API:coformer stoichiometry, crystallization solvent assuming actual manufacturing condition, and solvent vapor exposure temperature and time is sufficiently tolerable. This "enhanced nano-spot method" is applicable not only for cocrystal screening but also for the screening of API polymorphs or new crystalline forms (salts, solvates). In addition, introduction of a control stage of temperature or humidity enables further diversification of the crystallization conditions and is applicable to the thermal analysis and evaluation of moisture absorption/desorption behavior on a trace amount scale.

Because target APIs are now shifting from low-molecular-weight to medium- or high-molecular-weight APIs recently, the structure of API would be more complicated and expensive. Therefore, this method is expected to play a role in the pharmaceutical industry.

Funding

This work was supported in part by JSPS KAKENHI, Grant-in-Aid for Scientific Research (C), Grant Number 17K08253 (to T.F.).

Declarations of interest

The authors declared that there is no conflict of interest.

Appendix A. Supplementary material

Supplementary data to this article can be found online at https://doi.org/10.1016/j.ejpb.2019.01.018.

References

[1] N. Qiao, M. Li, W. Schlindwein, N. Malek, A. Davies, G. Trappitt, Pharmaceutical cocrystals: an overview, Int. J. Pharm. 419 (2011) 1–11.

[2] S. Aitipamula, R. Banerjee, A.K. Bansal, K. Biradha, M.L. Cheney, A.R. Choudhury, G.R. Desiraju, A.G. Dikundwar, R. Dubey, N. Duggirala, P.P. Ghogale, S. Ghosh, P.K. Goswami, N.R. Goud, R.R.K.R. Jetti, P. Karpinski, P. Kaushik, D. Kumar, V. Kumar, B. Moulton, A. Mukherjee, G. Mukherjee, A.S. Myerson, V. Puri, A. Ramanan, T. Rajamannar, C.M. Reddy, N. Rodriguez-Hornedo, R.D. Rogers, T.N.G. Row, P. Sanphui, N. Shan, G. Shete, A. Singh, C.C. Sun, J.A. Swift, R. Thaimattam, T.S. Thakur, R.K. Thaper, S.P. Thomas, S. Tothadi, V.R. Vangala, N. Variankaval, P. Vishweshwar, D.R. Weyna, M.J. Zaworotko, Polymorphs, salts, and cocrystals: what's in a name? Cryst. Growth Des. 12 (2012) 2147–2152.

[3] K. Izutsu, T. Koide, N. Takata, Y. Ikeda, M. Ono, M. Inoue, T. Fukami, E. Yonemochi, Characterization and quality control of pharmaceutical cocrystals, Chem. Pharm. Bull. (Tokyo) 64 (2016) 1421–1430.

[4] H. Yamashita, C.C. Sun, Improving dissolution rate of carbamazepine-glutaric acid cocrystal through solubilization by excess coformer, Pharm. Res. 35 (2017) 4.

[5] M. Yoshimura, M. Miyake, T. Kawato, M. Bando, M. Toda, Y. Kato, T. Fukami, T. Ozeki, Impact of the dissolution profile of the cilostazol cocrystal with supersaturation on the oral bioavailability, Cryst. Growth Des. 17 (2017) 550–557.

[6] J. Du, F. Lai, L. Váradi, P. Williams, P. Groundwater, J. Platts, D. Hibbs, J. Overgaard, Monoclinic paracetamol vs. paracetamol-4,4′-bipyridine co-crystal; what is the difference? A charge density study, Crystals 8 (2018) 46.

[7] S. Ranjan, R. Devarapalli, S. Kundu, V.R. Vangala, A. Ghosh, C.M. Reddy, Three new hydrochlorothiazide cocrystals: structural analyses and solubility studies, J. Mol. Struct. 1133 (2017) 405–410.

[8] N. Rodriguez-Hornedo, S.J. Nehm, K.F. Seefeldt, Y. Pagan-Torres, C.J. Falkiewicz, Reaction crystallization of pharmaceutical molecular complexes, Mol. Pharm. 3 (2006) 362–367.

[9] T. Friščić, W. Jones, Recent advances in understanding the mechanism of cocrystal formation via grinding, Cryst. Growth Des. 9 (2009) 1621–1637.

[10] V. Titapiwatanakun, A.W. Basit, S. Gaisford, A new method for producing pharmaceutical co-crystals: laser irradiation of powder blends, Cryst. Growth Des. 16 (2016) 3307–3312.

[11] N.K. Duggirala, M.L. Perry, Ö. Almarsson, M.J. Zaworotko, Pharmaceutical cocrystals: along the path to improved medicines, Chem. Comm. 52 (2016) 640–655.

[12] V. Luu, J. Jona, M.K. Stanton, M.L. Peterson, H.G. Morrison, K. Nagapudi, H. Tan, High-throughput 96-well solvent mediated sonic blending synthesis and on-plate solid/solution stability characterization of pharmaceutical cocrystals, Int. J. Pharm. 441 (2013) 356–364.

[13] T. Kojima, S. Tsutsumi, K. Yamamoto, Y. Ikeda, T. Moriwaki, High-throughput cocrystal slurry screening by use of in situ Raman microscopy and multi-well plate, Int. J. Pharm. 399 (2010) 52–59.

[14] S.R. Bysouth, J.A. Bis, D. Igo, Cocrystallization via planetary milling: enhancing throughput of solid-state screening methods, Int. J. Pharm. 411 (2011) 169–171.

[15] K. Nagapudi, E.Y. Umanzor, C. Masui, High-throughput screening and scale-up of cocrystals using resonant acoustic mixing, Int. J. Pharm. 521 (2017) 337–345.

[16] Y. Maeno, M. Inoue, T. Suzuki, K. Tomono, T. Fukami, Microanalysis of pharmaceutical cocrystals using a nano-spot method coupled with Raman spectroscopy, Cryst. Eng. Comm. 18 (2016) 8004–8009.

[17] C. Ji, M.C. Hoffman, M.A. Mehta, Catalytic effect of solvent vapors on the spontaneous formation of caffeine–malonic acid cocrystal, Cryst. Growth Des. 17 (2017) 1456–1459.

[18] K. Fujii, Y. Ashida, H. Uekusa, S. Hirano, S. Toyota, F. Toda, Z. Pan, K.D.M. Harris, Vapour induced crystalline transformation investigated by ab initio powder x-ray diffraction analysis, Cryst. Growth Des. 9 (2009) 1201–1207.

[19] S. Roy, B. Chamberlin, A.J. Matzger, Polymorph discrimination using low wavenumber Raman spectroscopy, Org. Process Res. Dev. 17 (2013) 976–980.

[20] P.J. Larkin, M. Dabros, B. Sarsfield, E. Chan, J.T. Carriere, B.C. Smith, Polymorph characterization of active pharmaceutical ingredients (APIs) using low-frequency Raman spectroscopy, Appl. Spectrosc. 68 (2014) 758–776.

[21] G. Walker, P. Romman, B. Poller, K. Lobmann, H. Grohganz, J.S. Rooney, G.S. Huff, G.P.S. Smith, T. Rades, K.C. Gordon, C.J. Strachan, S.J. Fraser-Miller, Probing pharmaceutical mixtures during milling: the potency of low-frequency raman spectroscopy in identifying disorder, Mol. Pharmaceut. 14 (2017) 4675–4684.

[22] C.J. Strachan, P.F. Taday, D.A. Newnham, K.C. Gordon, J.A. Zeitler, M. Pepper, T. Rades, Using terahertz pulsed spectroscopy to quantify pharmaceutical polymorphism and crystallinity, J. Pharm. Sci. 94 (2005) 837–846.

[23] J.A. Zeitler, D.A. Newnham, P.F. Taday, C.J. Strachan, M. Pepper, K.C. Gordon, T. Rades, Temperature dependent terahertz pulsed spectroscopy of carbamazepine, Thermochim. Acta 436 (2005) 71–77.

[24] G.M. Day, J.A. Zeitler, W. Jones, T. Rades, P.F. Taday, Understanding the influence of polymorphism on phonon spectra: lattice dynamics calculations and terahertz spectroscopy of carbamazepine, J. Phys. Chem. B 110 (2006) 447–456.

[25] T. Koide, T. Fukami, H. Hisada, M. Inoue, J. Carriere, R. Heyler, N. Katori, H. Okuda, Y. Goda, Identification of pseudopolymorphism of magnesium stearate by using low-frequency Raman spectroscopy, Org. Process Res. Dev. 20 (2016) 1906–1910.

[26] T. Otaki, Y. Tanabe, T. Kojima, M. Miura, Y. Ikeda, T. Koide, T. Fukami, *In situ* monitoring of cocrystals in formulation development using low-frequency Raman spectroscopy, Int. J. Pharm. 542 (2018) 56–65.

[27] M. Inoue, H. Hisada, T. Koide, J. Carriere, R. Heyler, T. Fukami, In situ monitoring of crystalline transformation of carbamazepine using probe-type low-frequency Raman spectroscopy, Org. Process Res. Dev. 21 (2017) 262–265.

[28] S.L. Childs, N. Rodríguez-Hornedo, L.S. Reddy, A. Jayasankar, C. Maheshwari, L. McCausland, R. Shipplett, B.C. Stahly, Screening strategies based on solubility and solution composition generate pharmaceutically acceptable cocrystals of carbamazepine, Cryst. Eng. Comm. 10 (2008) 856–864.

[29] D.R. Weyna, T. Shattock, P. Vishweshwar, M.J. Zaworotko, Synthesis and structural characterization of cocrystals and pharmaceutical cocrystals: mechanochemistry vs slow evaporation from solution, Cryst. Growth Des. 9 (2009) 1106–1123.

[30] M. Habgood, M.A. Deij, J. Mazurek, S.L. Price, J.H.T. Horst, Carbamazepine co-crystallization with pyridine carboxamides: rationalization by complementary phase diagrams and crystal energy landscapes, Cryst. Growth Des. 10 (2010) 903–912.

[31] V. Taresco, I. Louzao, D. Scurr, J. Booth, K. Treacher, J. McCabe, E. Turpin, C.A. Laughton, C. Alexander, J.C. Burley, M.C. Garnett, Rapid nanogram scale screening method of microarrays to evaluate drug-polymer blends using high-throughput printing technology, Mol. Pharm. 14 (2017) 2079–2087.